doi:10.1093/brain/awaa138 BRAIN 2020: 143; 1766–1779 | 1766

BRAIN
A JOURNAL OF NEUROLOGY

The role of the inferior parietal lobule in writer's cramp

Shabbir Hussain I. Merchant,[1,2] Eleni Frangos,[3] Jacob Parker,[1] Megan Bradson,[3] Tianxia Wu,[1] Felipe Vial-Undurraga,[1,4] Giorgio Leodori,[1,5] M.C. Bushnell,[3] Silvina G. Horovitz,[1] Mark Hallett[1] and Traian Popa[1,6,7]

Humans have a distinguishing ability for fine motor control that is subserved by a highly evolved cortico-motor neuronal network. The acquisition of a particular motor skill involves a long series of practice movements, trial and error, adjustment and refinement. At the cortical level, this acquisition begins in the parieto-temporal sensory regions and is subsequently consolidated and stratified in the premotor-motor cortex. Task-specific dystonia can be viewed as a corruption or loss of motor control confined to a single motor skill. Using a multimodal experimental approach combining neuroimaging and non-invasive brain stimulation, we explored interactions between the principal nodes of the fine motor control network in patients with writer's cramp and healthy matched controls. Patients and healthy volunteers underwent clinical assessment, diffusion-weighted MRI for tractography, and functional MRI during a finger tapping task. Activation maps from the task-functional MRI scans were used for target selection and neuronavigation of the transcranial magnetic stimulation. Single- and double-pulse TMS evaluation included measurement of the input-output recruitment curve, cortical silent period, and amplitude of the motor evoked potentials conditioned by cortico-cortical interactions between premotor ventral (PMv)-motor cortex (M1), anterior inferior parietal lobule (aIPL)-M1, and dorsal inferior parietal lobule (dIPL)-M1 before and after inducing a long term depression-like plastic change to dIPL node with continuous theta-burst transcranial magnetic stimulation in a randomized, sham-controlled design. Baseline dIPL-M1 and aIPL-M1 cortico-cortical interactions were facilitatory and inhibitory, respectively, in healthy volunteers, whereas the interactions were converse and significantly different in writer's cramp. Baseline PMv-M1 interactions were inhibitory and similar between the groups. The dIPL-PMv resting state functional connectivity was increased in patients compared to controls, but no differences in structural connectivity between the nodes were observed. Cortical silent period was significantly prolonged in writer's cramp. Making a long term depression-like plastic change to dIPL node transformed the aIPL-M1 interaction to inhibitory (similar to healthy volunteers) and cancelled the PMv-M1 inhibition only in the writer's cramp group. These findings suggest that the parietal multimodal sensory association region could have an aberrant downstream influence on the fine motor control network in writer's cramp, which could be artificially restored to its normal function.

1 National Institute of Neurological Disorders and Stroke, National Institutes of Health, Bethesda, MD, USA
2 Department of Neurology, Medical University of South Carolina, Charleston, SC, USA
3 National Center for Complementary and Integrative Health, National Institutes of Health, Bethesda, MD, USA
4 Facultad de Medicina, Clínica Alemana Universidad del Desarrollo, Santiago, Chile
5 IRCCS Neuromed, Pozzilli, IS, Italy
6 Defitech Chair of Clinical Neuroengineering, Center for Neuroprosthetics (CNP) and Brain Mind Institute (BMI), Swiss Federal Institute of Technology (EPFL), 1202 Geneva, Switzerland
7 Defitech Chair of Clinical Neuroengineering, Center for Neuroprosthetics (CNP) and Brain Mind Institute (BMI), Swiss Federal Institute of Technology Valais (EPFL Valais), Clinique Romande de Réadaptation, 1951 Sion, Switzerland

Received November 28, 2019. Revised March 1, 2020. Accepted March 9, 2020. Advance access publication May 18, 2020

Correspondence to: Shabbir Hussain I. Merchant
Assistant Professor of Neurology
Division of Movement Disorders
Medical University of South Carolina
208 B Rutledge Avenue, MSC 108
Charleston, SC 29425, USA
E-mail: merchash@musc.edu

Keywords: task-specific dystonia; writer's cramp; fine motor control; parietal lobe; cortical silent period

Abbreviations: a/dIPL = anterior/dorsal inferior parietal lobule; cSP = cortical silent period; CS-TS = conditioning stimulus-test stimulus; cTBS = continuous theta-burst stimulation; FDI = first dorsal interossei muscle; M1 = primary motor cortex; MEP = motor evoked potential; PMv = ventral premotor cortex; TMS = transcranial magnetic stimulation

Introduction

The skilful handling of objects is a distinguishing human ability. It is acquired over a long series of practice movements adjusted via multimodal sensory feedback. Our understanding of human fine motor control is mainly indirect, deriving inferences from studies of non-human primates, with additional insights gained from human neuroimaging studies (Rizzolatti and Luppino, 2001; Rizzolatti and Wolpert, 2005; Lemon, 2008*a*, *b*; Kristo *et al.*, 2014; Hamano *et al.*, 2020). The network implicated in human fine motor control, associated with pincer grasp involves the ventral premotor cortex (PMv) and anterior part of the inferior parietal lobule (aIPL) working in concert with the primary motor cortex (M1). The dorsal part of the inferior parietal lobule (dIPL) is the multimodal sensory association region, involved in the initial acquisition and learning of a motor task, which is subsequently stratified downstream in the fine motor control network composed of the aIPL-PMv-M1 (Rizzolatti and Luppino, 2001; Rizzolatti and Wolpert, 2005; Karabanov *et al.*, 2012). The selection of a particular motor sequence accounting for the object meaning, context and the desired goals of current actions are selected based on the inputs to PMv from the prefrontal cortex and parietal-temporal regions (Fagg and Arbib 1998; Grafton *et al.*, 1998; Rizzolatti and Luppino, 2001; Hamano *et al.*, 2020). The superior longitudinal fasciculus is the white matter pathway supporting these parietal-premotor interactions (Lemon, 2008*a*, *b*; Schaffelhofer and Scherberger, 2016).

The IPL is uniquely located and connected to many different brain regions, subserving several neurological processes. There are also distinctive connections and organization within the parietal lobe; however, the functional and behavioural implications of these interactions within the parietal lobe are poorly understood. The dIPL is posited to be the multimodal sensory association region and aIPL being one of the critical nodes of fine motor control network (Bremmer *et al.*, 2001; Rozzi *et al.*, 2008; Bonini *et al.*, 2010; Ishibashi *et al.*, 2011; Caspers *et al.*, 2013; Burks *et al.*, 2017; Deroche *et al.*, 2017; Bruni *et al.*, 2018).

Task-specific dystonia (TSD) has been defined as 'a collection of movement disorders that present with persistent muscular incoordination or loss of motor control during skilled movement' (Albanese *et al.*, 2013). Common forms include writer's cramp and musician's dystonia, both of which have been noted to involve functional alterations in fine motor skill circuits (Sadnicka *et al.*, 2016, 2018; Pirio Richardson *et al.*, 2017). Some of the pathophysiological mechanisms, such as loss of inhibition, abnormal plasticity, and abnormalities in sensorimotor integration are shared with other types of dystonia (Hallett, 2011; Quartarone and Hallett, 2013). In the context of human motor control, TSD can be viewed as a corruption of a specific aspect of a learned and perfected motor skill. This may initially manifest clinically as various degrees and patterns of difficulties in the performance of a particular task, which can potentially corrupt other learned motor skills over time, on account of maladaptive plasticity (Sadnicka *et al.*, 2018). It is also recognized today that abnormal input from subcortical structures contribute to the abnormal cortical plasticity and motor learning, which supports the view that TSD is a network disorder (Peterson *et al.*, 2010; Shakkottai *et al.*, 2017; Kaji *et al.*, 2018).

Previous studies on TSD have reported abnormally increased activation in the dIPL region (Gallea *et al.*, 2016; Battistella and Simonyan, 2019; Bianchi *et al.*, 2019). Considering dIPL from the perspective of motor learning, it could be considered a prime candidate for the introduction and maintenance of aberrancies within the fine motor control network (Karabanov *et al.*, 2012; Gallea *et al.*, 2016; Battistella *et al.*, 2017; Battistella and Simonyan, 2019; Bianchi *et al.*, 2019). If this were the case, transiently lowering the responsiveness of this region could lead to the normalization of its downstream influence on the fine motor control network.

In humans, network-level pathophysiological interactions can be probed, and excitability temporarily altered using non-invasive brain stimulation techniques such as simple and repetitive transcranial magnetic stimulation (TMS). The excitability of M1 can be quantified indirectly with the amplitude of motor evoked potentials (MEP) and the duration of cortical silent periods (cSP) by single pulses: the recruitment curve can reveal the threshold, as well as the excitability

profile of M1, while the cSP can give a measure of the speed with which the motor circuits can resume their normal interaction after an artificially-induced focal disruption (Chen *et al.*, 1997; Classen *et al.*, 2000; Cantello, 2002; Saisanen *et al.*, 2008). The functional influence of other cortical areas onto M1 can be quantified with MEP by paired TMS pulses—one pulse delivered over an area of interest influencing M1 followed by a second pulse delivered over M1. Aberrancies in these interactions can provide useful pathophysiological insights into disorders of motor control (Rizzolatti and Luppino, 2001; Davare *et al.*, 2008; Lemon 2008*a*, *b*). The preponderant normal and dystonic interactions within the fine motor control network, probed using paired pulse TMS are summarized in Fig. 1. Techniques utilizing repetitive TMS can be used to influence cortical excitability by inducing a temporary long-term potentiation-like (LTP-like) or long-term depression-like (LTD-like) plastic change. Theta-burst stimulation (TBS) is one such high frequency repetitive stimulation paradigm used to transiently alter the excitability of a brain region, which can potentially influence the involved network (Huang *et al.*, 2005; Wischnewski and Schutter, 2016)

In this exploratory study, we used a multimodal approach combining structural and functional MRI, and TMS to quantify the interactions between the principal cortical nodes of fine motor control network in patients with writer's cramp and matched healthy controls. We also explored whether artificially decreasing the excitability of the dIPL would have any direct influence on M1 excitability and its interactions within the fine motor control network. The focus of this study was to explore the interactions within the cortical fine motor control network readily accessible to TMS, leaving subcortical structures out of the model (Hubsch *et al.*, 2013). To address these exploratory aims we recruited participants with writer's cramp and healthy volunteers, and asked the following questions: (i) Do patients with writer's cramp and control subjects differ in structural and resting state functional connectivity between the cortical hubs of fine motor control? (ii) Do patients with writer's cramp and control subjects differ in cortical excitability? (iii) Do patients with writer's cramp have altered physiological interactions within the fine motor control network, while at rest? and (iv) Would transiently decreasing the excitability of the dIPL have any direct influence on motor cortical excitability and/or downstream influence on the fine motor cortical excitability and/or downstream influence on the fine motor control network? To address these questions, we carried out diffusion weighted imaging (DWI) for tractography, a resting state functional MRI to assess functional interactions at rest, a finger tapping task functional MRI scan for neuronavigation purposes, and explored the interactions within the cortical parieto-premotor-motor network (aIPL/dIPL-PMv-M1) at baseline and after modulating the excitability of dIPL by inducing an LTD-like plastic change with continuous TBS (cTBS), in a randomized sham-controlled design.

Materials and methods

Participants

Nine patients with writer's cramp based on clinical criteria (Albanese *et al.*, 2013), affected on their right side (four females) and 15 healthy volunteers (five females), without any other

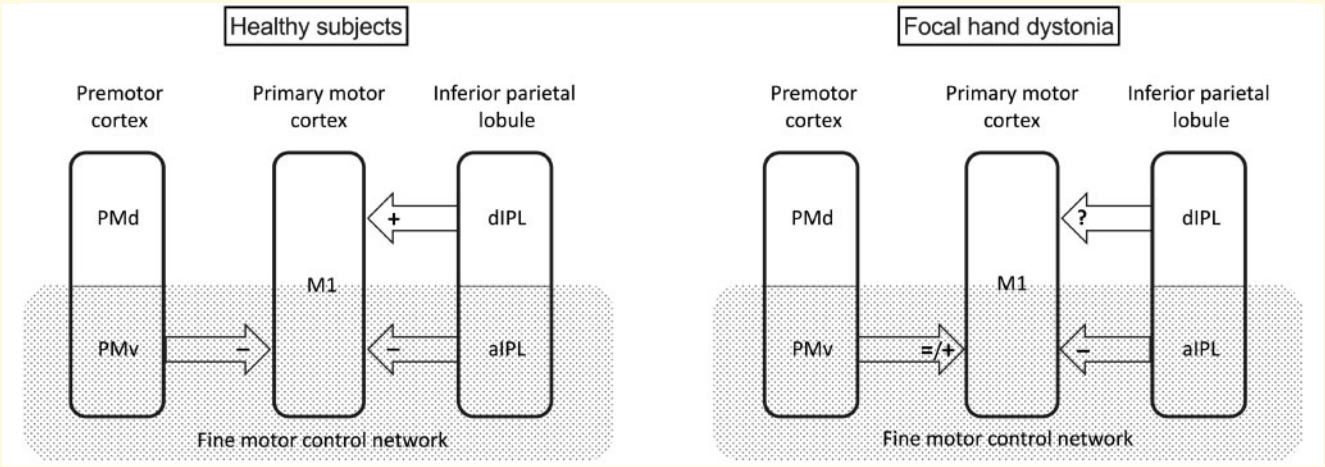

Figure 1 Schematic representation of the principal cortical nodes involved in human upper limb fine motor control, as they emerge from previous studies. The fine motor control network involved in pincer grasp is composed of aIPL, PMv, and M1. Predominant interactions between the different regions implicated in upper limb motor control using TMS-based cortico-cortical interactions using a conditioning stimulus-test stimulus (CS-TS) paradigm as noted in healthy subjects and focal hand dystonia. Inhibitory interactions are reflected by a reduced amplitude of the MEPs after a double pulse, while excitatory interactions are reflected by an increased amplitude of the MEPs, both when compared with MEPs of single pulses delivered over M1. Inhibitory PMv-M1 interactions have been reported in healthy volunteers and loss of PMv-M1 inhibition reported in focal hand dystonia. Inhibitory aIPL-M1 interactions have been reported in healthy volunteers and focal hand dystonia. Facilitatory dIPL-M1 interactions have been reported in healthy volunteers and are unknown in focal hand dystonia.

neurological or psychiatric disorders were enrolled in this exploratory study. The clinical assessment included neurological examination and scoring of the dystonia on the Burke-Fahn-Marsden Dystonia Rating Scale (BFMDRS) (Burke *et al.*, 1985). Subjects on chronic opioid, anticholinergic or GABA-ergic medications, or reported alcohol consumption of >14 drinks/week were excluded. Patients being treated with botulinum toxin injections were studied at least 3 months after their last injections. The study was approved by the Combined Neurosciences Institutional Review Board of the National Institutes of Health (NIH).

Experimental design

Study overview

Subjects satisfying the study inclusion criteria underwent the initial clinical assessment. Subsequently, they underwent a clinical MRI, to verify subjects had no pathological findings, T_1-weighted images for image registration, DWI for tractography and evaluation of structural connectivity, functional MRI during rest to evaluate resting state functional connectivity, and functional MRI during a finger tapping task between the index and thumb for target localization. Single subject functional MRI activation maps of the motor control network mapped onto their anatomical scans were used for target selection and TMS neuronavigation. Baseline TMS evaluation included measurement of input-output recruitment curve (IOC) and cSP to evaluate cortical excitability, and the variation in the amplitude of MEPs conditioned by cortico-cortical interactions between PMv-M1, aIPL-M1 and dIPL-M1 to evaluate physiological connectivity. After the baseline block, one cTBS block of 600 pulses was applied to the dIPL node. The cTBS is a non-invasive brain stimulation technique capable of inducing a temporary LTD-like plastic change in the superficial cortical areas (Huang *et al.*, 2005; Wischnewski and Schutter 2016). Either real or sham cTBS (randomized and counterbalanced) was applied at two separate sessions to all subjects, with at least 24 h between the two sessions. After the cTBS block, the same parameters recorded at baseline were re-evaluated to ascertain the influence of making an LTD-like plastic change to dIPL on cortical excitability and downstream physiological interactions within the fine motor control (aIPL-PMv-M1) network. The dIPL-M1 interaction was not tested after cTBS, since the cTBS intervention was applied to dIPL node and the overarching exploratory hypothesis was to study the influence of a plastic change of this node downstream on the fine motor control network. The overview of the study design is presented in Fig. 2.

Structural and functional MRI

MRI acquisition

Brain images were acquired using a 3 T Siemens Skyra scanner (Siemens) with a 32-channel head coil. Details of the MRI acquisition parameters are noted in the Supplementary material.

Scanning procedures

Participants completed a series of scans as indicated in Fig. 2A. Subjects wore earplugs throughout the session and their heads were immobilized with foam padding. Finger movements were monitored during scans with functional MRI compatible EMG recording electrodes placed on the right first dorsal interossei muscle (FDI). The right hand was positioned in a comfortable, rested, supinated position along the right side of the body.

Resting state and task scans

A 6-min resting state scan was collected prior to the task scans. Participants were instructed to relax, keep their eyes open, and fixate on a white cross hair on a black screen for the duration of the scan.

Each of the two subsequent task scans began with a 1-min rest period followed by counterbalanced 18-s blocks of 'Tap' and 'Imagine tapping' (five trials per block, two blocks per condition), each followed by a 'Rest' block (jittered 8–14 s). Participants tapped their right index finger to their right thumb (a pincer-like motion) at a rate of ~1–2 Hz or imagined doing the action, respectively. The fine motor 'pincer' tapping, the tapping rate, and imagining the action were rehearsed prior to the scanning session. Following each block of trials, two pain intensity scales were presented for 10 s. They are described in the Supplementary material and not used in the analysis.

Functional MRI preprocessing and analysis

All data were preprocessed using FSL version 6.00 (FMRIB Software Library, Oxford, UK). Briefly, preprocessing included removal of the skull and non-brain tissue, standard motion correction (six parameters), grand-mean intensity normalization of all voxels across time, high-pass filtering, and spatial smoothing using a Gaussian kernel of fixed-width at half-maximum (FWHM) = 5 mm and 6 mm for the task and resting state data, respectively. Further preprocessing of the resting state data included single session independent components analysis (ICA) using MELODIC (version 3.14) with automatic dimensionality estimation. Artefacts were identified using FMRIB's ICA-based Xnoisefier (FIX 1.06;) and then regressed from each individual's resting state data. The classification threshold was set to 20. Registration of the task functional image to the individual's anatomical was performed using a six parameter registration, followed by a 12-parameter linear registration to the MNI152 standard space template. A non-linear registration to standard space was carried out for the resting state functional data. Details are provided in the Supplementary material.

Task scan analyses

The task scan data were analysed prior to the TMS session and used for the functional neuro-navigation procedures. At the individual level, explanatory variables (EV) for the 'tapping' and 'imagine' conditions were created for each of the two runs and modelled using a double-gamma haemodynamic response function. Rest periods were not included in the model. A fixed-effects, whole-brain analysis was used to average the 'tapping' conditions across both runs for each individual. The peak uncorrected, linearly registered results observed in each individual's finger tapping activation map were used to localize the four subject-specific nodes (left dIPL, aIPL, M1, and PMv).

Seed-based resting state analysis

To assess the functional connectivity between the four nodes of interest (left dIPL, aIPL, M1, and PMv) during resting state, we extracted the time series from 6 mm spheres (seeds) created based on the peak activity observed in the finger tapping task. Each sphere was confirmed to be within the respective

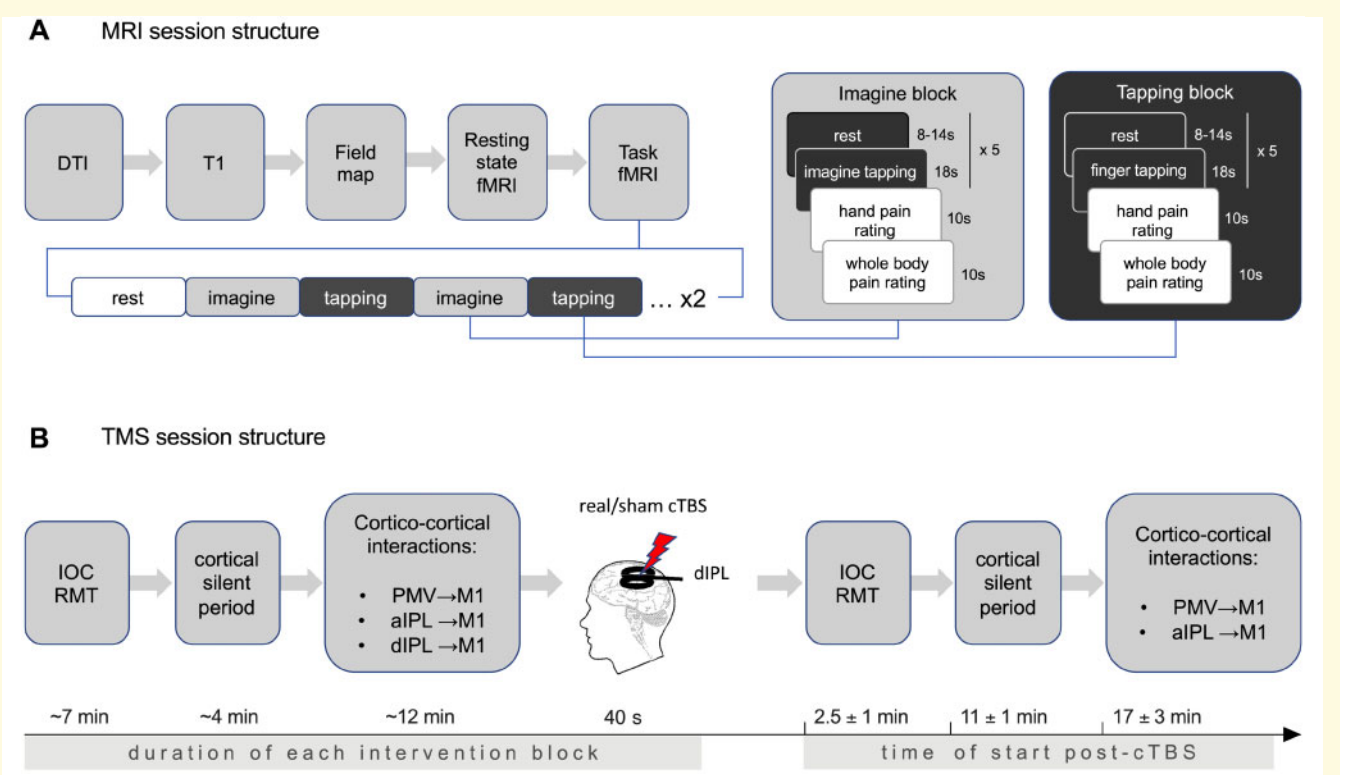

Figure 2 Experimental procedures. (**A**) Each scanning session included diffusion tensor imaging (DTI), high resolution anatomical MRI, field mapping, resting state functional MRI (fMRI), and two task-based functional MRI scans to assess neural responses during tapping of the right index finger to the thumb, or imagining this movement. The order in which the 'tapping' and 'imagine' blocks were presented was counterbalanced between the two scans. (**B**) TMS experiment involved baseline recording of input-output recruitment curve (IOC), resting motor threshold (RMT), cortical silent period (cSP), and cortico-cortical interactions between PMv-M1, aIPL-M1, and dIPL-M1. A block of real/sham cTBS was applied to the dIPL node followed by repeated measurements of IOC, RMT, cSP, and cortico-cortical interactions between PMv-M1 and aIPL-M1. The approximate timelines for the performance of the different TMS experimental blocks pre- and post-cTBS are also noted.

anatomical region based on the Juelich Histological Atlas (Supplementary Fig. 1). This atlas was used to create four regions of interest for the small volume correction seed-based analysis. The PFm and PGa parcellation of the IPL made up the dIPL mask, and the PFop parcellation of the IPL made up the aIPL mask (Economo and Koskinas, 1925; Caspers *et al.*, 2013). The M1 mask was restricted to the region of the hand representation, and the PMv mask was restricted to the PMv region identified by the Mayka *et al.* (2006) meta-analysis.

DTI preprocessing and data analysis

The DWIs were processed using TORTOISE and FATCAT software with the default parameters (Pierpaoli, 2010; Taylor and Saad, 2013; Irfanoglu *et al.*, 2017). Raw volumes were visually inspected and removed if significant motion was present. Motion and eddy current distortion corrections were performed on the A-P and P-A datasets independently within the diffprep module then corrected for EPI distortion using DR-BUDDI. The two datasets were registered to an axial T_2-weighted image and non-linear tensor estimation was carried out on the final DWIs using FATCAT.

The probabilistic tractography was performed using the 3dTrackID program in FATCAT, which carries out repeated iterations of whole brain tracking to estimate the likelihood of structural white matter connections between all pairs of target regions of interest within the predefined network (Saad and Reynolds, 2012; Taylor and Saad, 2013). The same spheres of M1, PMv, aIPL, and dIPL from the functional analysis were used as the regions of interest for the tractography. Prior to tractography, each region of interest was inflated by a maximum of two voxels until its surface was directly adjacent to the white matter skeleton defined by a fractional anisotropy (FA) > 0.2. Tractography was performed between each possible region of interest pair.

TMS neuro-navigational set-up

Each individual set of MRI scans was uploaded to a frameless stereotaxic neuro-navigation system (Brainsight2; Rogue Research, Montreal, Quebec, Canada), which allows simultaneous neuro-navigation of two TMS coils. The sets consisted of three images linearly registered to the MNI template space: the T_1-weighted (with skull) for 3D head reconstruction, its skull stripped version for functional MRI registration, and the uncorrected activation map from the finger tapping task for targeting M1, PMv, aIPL, and dIPL. The functional MRI activation within each pre-defined area of interest from single subject data

were used as TMS targets for each individual. The precise coordinates of these hotspots and the mismatch between the anatomically and functionally defined stimulation targets can be found in Supplementary Table 2 and Supplementary Fig. 2, respectively. A clear activation of the aIPL, PMv and M1 nodes was noted in all subjects. In the rare cases when dIPL activation was not clearly noted, the centroids of the anatomical regions of interest were selected from the atlas mapped to the individual anatomy. The M1 hotspot (site and coil orientation giving most consistently the highest MEP at the lowest stimulator output) for FDI was determined empirically and the coil oriented to induce the current in a posterior-anterior direction within M1. The motor hotspot determined empirically with the TMS and used for the experiment overlapped with the M1 hotspot indicated by the functional activation mask during finger tapping task in all subjects, further confirming good alignment of the overlays used for neuro-navigation.

EMG set-up

Participants were seated in a comfortable armchair with the right arm rested on a pillow. The EMG activity of the right FDI (muscle of interest) was recorded throughout the experiment. Ag-AgCl surface electrodes were placed in a belly-tendon montage, with impedances kept below 20 kΩ. Data were collected using a Viking IV EMG machine (Nicolet Biomedical), bandpass filtered at 20–2000 Hz with the amplified (1000×) analogue outputs digitized at 5 kHz with the Signal software (version 5.09; Cambridge Electronic Design, Cambridge, UK) and stored in a computer for offline analysis.

TMS input-output recruitment curve and cortical silent period

Input-output curve

The resting motor threshold (RMT), S50 (stimulation intensity required to obtain a peak-peak EMG response at 50% of the maximum), and slope of an input-output curve (IOC) are variables that can reflect motor cortical excitability. The slope of the IOC can also reflect lability and variability of motor cortical excitability. To obtain these measures, TMS was applied tangentially to the scalp over the left M1 hand area, with the *x*-axis parallel to the central sulcus and the *y*-axis oriented to induce a posterior-anterior current flow in the brain. The optimal site and coil orientation for evoking MEPs from the contralateral FDI muscle was identified as the motor hotspot.

The IOC was obtained by giving 60 single pulses of different intensities (three pulses for each 5% increment between 5% to 100% of the maximal stimulator output), via a custom-made, 'branding ion' style figure-of-eight coil (70 mm outer diameter) linked to a monophasic Magstim 200^2 module. The data were fitted with a Boltzmann sigmoidal function. The S50 for FDI was determined from the fitted IOC and used as the test stimulus (TS) intensity throughout the experiment. The RMT was determined as the lowest intensity that induced 50 μV peak-to-peak amplitude MEP in 5 of 10 trials from the motor hotspot. The conditioning stimulus (CS) intensity used for the experiment was 90% of the RMT.

Cortical silent period

The cSP is defined as the time required for re-emergence of ongoing tonic EMG activity in a muscle after interruption using a single TMS pulse producing a MEP. The duration of the cSP has been associated with GABAergic inhibition and proposed to correlate with cortical excitability (Saisanen *et al.*, 2008); shortening of the silent period deemed to be reflective of loss of inhibition. The subject's right hand was secured on a manipulandum in prone position, only allowing abduction of FDI with the right index finger over a force transducer (Supplementary Fig. 3A). The subject's maximal voluntary contraction (MVC) was determined as the maximal force generated by holding the FDI in tonic contraction for 5 s. The subject was then asked to hold the FDI in tonic contraction at a constant force between 30–50% of MVC while visual feedback was provided on a potentiometer. For the measurement of cSP, the subjects maintained this constant tonic contraction of the right FDI while 20 TMS pulses (divided into two blocks of 10 pulses) were delivered over the motor hotspot at S50. The cSP was measured as the duration of interruption of the ongoing EMG motor activity after each individual pulse, beginning from the TMS artefact and ending with the resumption of the tonic FDI activity. The individual 20 measurements were then averaged for each subject and submitted to the group statistical analysis. Identical cSP measurements were performed before and after the cTBS block (both real and sham).

Dual site TMS

To compare the interactions within the fine motor control network in writer's cramp patients and healthy volunteers, we studied the physiological interactions between PMv-M1, aIPL-M1 and dIPL-M1, with nodes defined functionally by each individual's finger tapping activation map (Supplementary Fig. 2). Custom-made, figure-of-eight, 'branding iron' style coils with 70-mm external diameter were used. Stimulation was delivered using two high-power, monophasic Magstim200^2 stimulators (Magstim Company Ltd.).

For the PMv-M1 stimulation block, conditioning stimulus coil was initially placed centred on the functional PMv node, with the coil placed in an anterior-posterior and slight lateral-medial orientation towards M1. For the aIPL-M1 and the dIPL-M1 stimulation the conditioning stimulus coil was placed first in a posterior-anterior orientation. The TS M1 coil was then placed to be centred on the motor hotspot with the coil oriented in the posterior-anterior direction; the coil trajectory modified in order to accommodate both the coils, which overlapped slightly (Supplementary Fig. 3B). After the coil positions were secured, trial pulses were delivered to ensure clear MEPs with the target peak-peak amplitude close to the S50 amplitude. The stimulator output intensity was increased to obtain the target MEP amplitude if the coil orientation needed to be changed in order to accommodate both coils. After the coil position and stimulator outputs were optimized, the coil trajectories were saved for the post-cTBS block.

The interstimulus interval (ISI) used for studying these cortico-cortical interactions were defined based on the nature of the connections between these nodes; premotor cortex having a direct projection to M1 whereas the parietal cortex mainly having an indirect projection to M1 via the premotor cortex. They are also explained based on the latency of the late I (indirect) waves generated by TMS, where these cortico-cortical interactions

occur (Rizzolatti and Luppino, 2001; Cerri *et al.*, 2003; Shimazu *et al.*, 2004; Koch *et al.*, 2008; Baumer *et al.*, 2009; Karabanov *et al.*, 2013; Schaffelhofer and Scherberger, 2016; Bruni *et al.*, 2018). Therefore, for the PMv-M1 block, 30 MEPs were collected: 10 after single pulses, 10 each after CS-TS pulse pairs with 4 ms and 6 ms ISI. For the aIPL-M1 and dIPL-M1 blocks 30 MEPs were collected for each: 10 after single pulses, 10 each after CS-TS pulse pairs with 6 ms and 8 ms ISI. Pulses were delivered in a randomized order.

Inhibition of the dorsal inferior parietal lobule using continuous TBS

To assess downstream effects of inducing LTD-like plastic change (inhibition) in the dIPL onto cortical excitability and fine motor control network, we used a cTBS 600 protocol involving triplets of pulses at 50 Hz repeated at a frequency of 5 Hz resulting in 600 pulses over 40 s (Huang *et al.*, 2005). The cTBS was applied using the Magstim Rapid^2 and AirFilm Coil [average coil diameter of $2\times$ (3×0.92 mm)] that delivered biphasic pulses of 0.5 ms duration with an average rise time of ~80 ms (Magstim Company Ltd.). The RMT was measured using this coil and 80% of RMT was used as the stimulation intensity for cTBS. The same dIPL target used for the dIPL-M1 CS-TS block was used for cTBS. The coil was orientated tangentially over the scalp to induce a PA current for the real cTBS block. For the sham block, the coil edge was held on target with the coil centre facing posteriorly and perpendicular to the scalp.

Statistical analysis

Demographics

Differences between the writer's cramp and healthy volunteer groups for age, gender and handedness were examined using a two-sample *t*-test (continuous variable with normal distribution), Mann-Whitney test (continuous variable with abnormal distribution), or Fisher's exact test (binary variable). The assumption of normality was tested using the residuals and Shapiro-Wilk method.

Resting state seed-based

A mixed effects model (FLAME 1) was used to evaluate group connectivity differences between each node pair. The model included the following contrasts: healthy volunteers > writer's cramp; writer's cramp > healthy volunteers; mean healthy volunteers connectivity; and mean writer's cramp connectivity. All analyses were corrected for age (mean-centred across all participants). Voxel-based thresholds were set to $z > 2.3$ and were cluster corrected for multiple comparisons at $P < 0.05$. Correlations between clinical measures and functional MRI data were investigated using Pearson correlations.

Diffusion tensor imaging

A two-sample *t*-test was used to examine the difference in structural connectivity (fractional anisotropy). Age was not used as a covariate considering the low correlation between age and fractional anisotropy for the cohort.

Electrophysiology

The conditioned MEP amplitudes of the dual-site paradigms were normalized to the mean amplitude of the unconditioned MEPs during the same experimental block.

To evaluate the reliability of cSP measurement, intraclass correlation coefficients were calculated for writer's cramp and healthy volunteers separately using the three repeated measures from each subject: pre-intervention for both real and sham and post-intervention for sham only.

For each of the three outcome measures: cSP, PMV-M1 and alPL-M1, repeated measures ANOVA was performed to evaluate the effect of Group (writer's cramp versus healthy volunteers), Intervention (real versus sham), and Time (pre- versus post-intervention), and their interactions (Group × Intervention, Group × Time, Intervention × Time, and Group × Intervention × Time). Group was a between-subject factor, and both intervention and time were within-subject factors. Since the study design involved two within-subject factors, covariance structure un@cs (un: unstructured for intervention, cs: compound symmetry for time) was used to address the covariance within the subject, where the time was nested within intervention.

For the outcome measure of dIPL-M1, repeated measures ANOVA was performed to evaluate the effect of group (writer's cramp versus healthy volunteers), where the means of the outcome measure from two sessions were used as dependent variable, since the repeated measures were similar (paired *t*-test $P > 0.5$ for TSD and healthy volunteers group).

The reported *P*-values were adjusted (Holm's adaptive method) for multiple comparisons for each experiment, but not for the multiple ($n = 4$) experiments. Significance level (α) of 0.05 was used for the comparison of means, and $\alpha = 0.1$ for interaction test. Statistical analyses were performed with SAS version 9.4.

Data availability

The data that support the findings of this study are available from the authors upon reasonable request.

Results

Demographic characteristics and experimental timelines

Twelve healthy volunteers and nine patients with writer's cramp completed all the experiments and were included in the final analyses. Of the 15 healthy volunteers recruited, three were excluded from the final analysis; two did not return for the second TMS session and one had high motor thresholds and could not tolerate the intensity of TMS. For one patient with writer's cramp, cSP data for the post-cTBS cSP block could not be correctly analysed on account of artefactual errors and were excluded. No significant unexpected adverse events were reported. Both groups were similar in terms of age, gender, and handedness (Table 1). All writer's cramp patients had dystonia of the right hand only for the task of writing and no other fine motor dexterity

Table 1 Comparative demographic and clinical characteristics of healthy volunteers and writer's cramp cohort

	Healthy volunteers *n* = 12	Writer's cramp *n* = 9	*P*-value
Age, median; 25–75th quartiles	43.3; 31.5–51.25	58; 48–60	0.11[a]
Gender, male/female	7/5	5/4	1.0[b]
Handedness, right/left/ambidextrous	11/0/1	7/1/1	0.70[b]

[a]Mann-Whitney test.
[b]Fisher's exact test.

Table 2 Demographic and clinical characteristics of the writer's cramp cohort

Subject ID	Age	Sex	Handedness	Dystonic hand	BFMDRS scores		Disease duration, years
					Right arm	Left arm	
SJ201	44	M	Right	Right	4	0	3
SJ202	65	M	Right	Right	4	0	25
SJ203	59	M	Right	Right	4	0	18
SJ204	66	F	Left	Both	4	6	26
SJ205	58	F	Right	Right	4	0	20
SJ206	37	F	Ambidextrous	Both	6	4	5
SJ207	48	M	Right	Right	4	0	11
SJ208	57	F	Right	Both	6	4	13
SJ209	60	M	Right	Right	6	0	8

BFMDRS = Burke-Fahn-Marsden Dystonia Rating Scale.

issues (Table 2). The average time between the two experimental sessions when the real cTBS was performed first was 12 days (range 2–27 days). The TMS coordinates of the nodes for the two groups and the average duration of the post-TBS experimental blocks are provided in Supplementary Table 1.

Patients with writer's cramp have altered functional and normal structural connectivity

The seed-based resting state analysis indicated that each nodal pair in both groups had a significant positive correlation (Supplementary Table 2). However, the functional connectivity between dIPL-PMv was significantly greater in patients with writer's cramp compared to healthy controls (Fig. 3 and Supplementary Table 2). There was no relationship between the dIPL-PMv connectivity in writer's cramp patients and their symptom severity ($r = 0.23$, $P = 0.55$) or their symptom duration ($r = 0.06$, $P = 0.87$). No other resting state functional connectivity group differences were observed.

The tractography algorithm found white matter connections in at least 75% of subjects of each group (7/9 writer's cramp and 12/15 healthy volunteers) only for the PMv-M1, aIPL-PMv, and dIPL-PMv node pairs, and in $<50\%$ for the other node pairs (aIPL-M1 and dIPL-M1). We found no significant group differences in the white matter integrity of the pathways connecting the nodes of interest involved in fine motor control. The mean fractional anisotropy values ± standard deviation (SD) between the nodes for each group were: M1-PMv (healthy volunteers 0.45 ± 0.02, writer's cramp 0.45 ± 0.02; $P = 0.8$); PMv-aIPL (healthy volunteers 0.43 ± 0.03, writer's cramp 0.41 ± 0.03; $P = 0.1$); PMv-dIPL (healthy volunteers 0.47 ± 0.03, writer's cramp 0.47 ± 0.03; $P = 0.6$).

Prolonged cortical silent period and normal recruitment curves in writer's cramp

No significant differences were noted between the healthy volunteers and writer's cramp cohort in terms of baseline S50 values ($P = 0.78$). This did not change after either the real or sham $cTBS_{dIPL}$ in the healthy volunteers ($P = 0.87$) or writer's cramp ($P = 0.98$) group.

The cSP was found to be significantly longer in the writer's cramp cohort compared to the healthy volunteers [$F(20.4)$; $P < 0.0001$] (Fig. 4B). The intraclass correlation coefficient (ICC) for the three measures of cSP within the same subjects for each group separately suggested good reproducibility and reliability [ICC = 0.60, 95% confidence interval (CI): 0.19–0.89, for writer's cramp and ICC = 0.62, 95% CI: 0.30–0.86 for healthy volunteers]. Combining the two groups for the entire cohort of total 20 subjects, ICC = 0.79, 95% CI: 0.62–0.90 (Shrout and Fleiss 1979). A mixed model ANOVA revealed a slight increase in cSP for both the healthy volunteers and writer's cramp groups after $cTBS_{dIPL}$, but no other new significant effects or interactions (Table 3). This symmetrical prolongation of cSP in the two groups post-cTBS could be an effect of time (i.e. fatigue) and not related to the intervention *per se*.

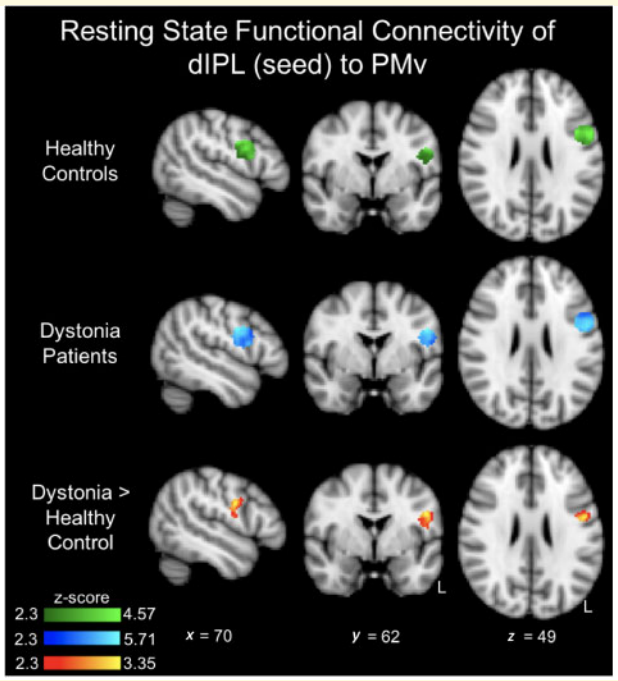

Figure 3 Results of dIPL connectivity to PMv. Each group had significant dIPL-PMv functional connectivity (green and blue). However, patients with writer's cramp had greater dIPL-PMv functional connectivity compared to healthy controls (red-yellow). Results are corrected for age and presented using a cluster-forming threshold of $z > 2.3$ and a cluster-corrected threshold of $P < 0.05$.

Normal PMv-M1 inhibition in writer's cramp

Using normalized MEP amplitudes evoked by the CS-TS paradigm as a dependent variable, no significant between-group differences were noted for the baseline PMv-M1 interactions. A similar degree of inhibition was noted for the CS-TS paradigm at baseline for the two groups (baseline between group difference, $t = 0.35$; $P = 0.73$; normalized MEP ± SD, healthy volunteers 0.87 ± 0.15; $t = -3.87$; $P = 0.0003$; writer's cramp 0.85 ± 0.16; $t = -3.49$; $P = 0.0013$) (Fig. 5A).

Loss of aIPL-M1 inhibition and dIPL-M1 facilitation in writer's cramp

Using normalized MEP amplitudes evoked by the CS-TS paradigm as a dependent variable, significant between-group differences were noted for the baseline aIPL-M1 interactions. The baseline aIPL-M1 interaction showed significant inhibition only for the healthy volunteers group (baseline between group difference, $t = -2.3$; $P = 0.02$; normalized MEP ± SD, healthy volunteers 0.89 ± 0.16; $t = -2.5$; $P = 0.016$; writer's cramp 1.01 ± 0.14; $t = 0.62$; $P = 0.54$) (Fig. 5B).

Using normalized MEP amplitudes evoked by the CS-TS paradigm as a dependent variable, significant between-group differences were noted for the baseline dIPL-M1 interactions ($F = 28.61$; $P < 0.0001$) compared to TS alone. The baseline dIPL-M1 interaction was notable for significant facilitation (baseline average normalized MEP ± SD = 1.13 ± 0.19; $t = 3.43$; $P = 0.0013$) for the healthy volunteers group while displaying significant inhibition for the writer's cramp group (baseline average normalized MEP ± SD = 0.849 ± 0.13; $t = -4.69$; $P = 0.00004$). The results are suggestive of opposite influence of the dIPL on M1 for the two groups ($t = 5.46$; $P < 0.00001$) (Fig. 5C and Table 3).

Effect of continuous TBS of the dIPL on the aIPL-PMv-M1 network

No changes were observed in the baseline PMv-M1 interactions in the healthy volunteers group after cTBS of dIPL. There was a loss of baseline PMv-M1 inhibition for the writer's cramp group, only for the real intervention (Fig. 5A). ANOVA revealed significant effects of the factor Time ($F = 6.5$; $P = 0.018$) and significant interactions Group × Time and Group × Time × Intervention (Table 3). The Bonferroni adjusted P-value (Holm's correction) was significant only for the real intervention in the writer's cramp group ($P = 0.0012$) and not for the sham intervention ($P = 0.97$).

Continuous TBS of the dIPL node did not alter significantly the baseline aIPL-M1 interactions for the healthy volunteers group (Fig. 5B). Mixed model ANOVA revealed a significant change post-cTBS in the writer's cramp group, with aIPL-M1 interaction now being significantly inhibitory compared to baseline. ANOVA revealed significant interactions for Group × Time and Group × Time × Intervention (Table 3). The *post hoc* analysis, showed that the Bonferroni adjusted P-value (Holm's correction) was significant only for the real intervention in the writer's cramp group ($P = 0.045$) and not for the sham intervention ($P = 0.83$).

Discussion

Using a multimodal experimental approach combining non-invasive brain stimulation and neuroimaging, we explored the physiological, functional and structural interactions between the principal cortical nodes involved in human fine motor control in a cohort of task-specific dystonia with writer's cramp compared to healthy volunteers. The evaluation of cortico-cortical interactions between the parietal and premotor areas implicated in fine motor control using neuronavigation based targeting of each individual's relevant functional network is a novel personalized approach for movement disorders. Our exploratory hypothesis was that possible abnormalities in the parietal sensorimotor integration regions might have aberrant downstream influence on the fine motor control network resulting in corruption of a

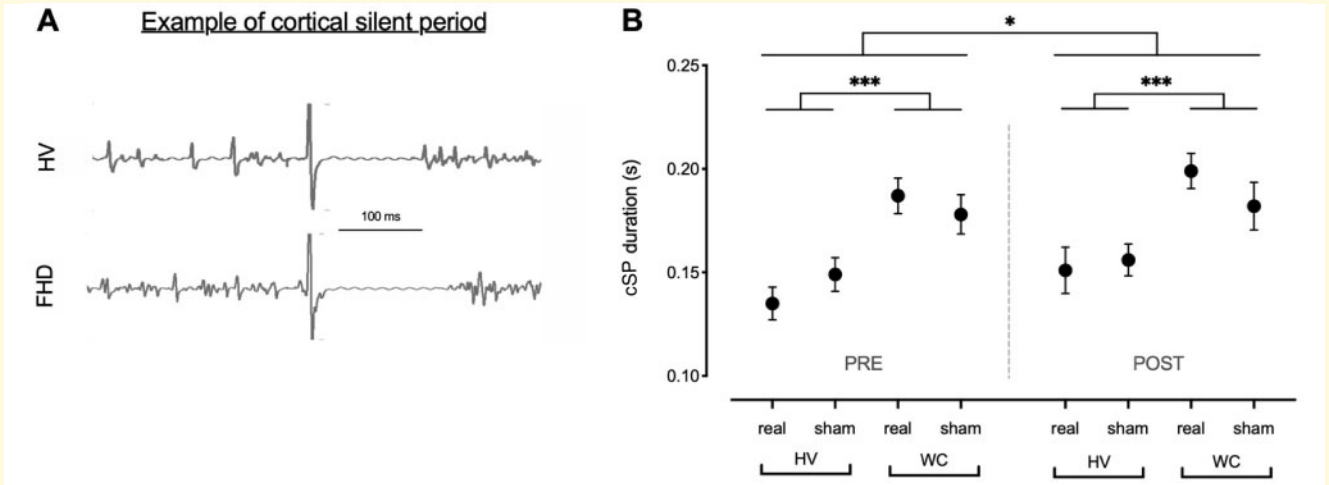

Figure 4 Summary of cSP results. (**A**) Example of cSP in healthy volunteers (HV) and writer's cramp (WC), demonstrating interruption in ongoing muscle EMG activity after a TMS pulse resulting in an MEP with re-emergence of EMG activity noted after a period of EMG silence, which is defined as the cSP. The duration of the cSP being notably longer in writer's cramp. (**B**) Summary of cSP results at baseline and post-intervention (real versus sham), demonstrating significantly prolonged cSP at baseline in writer's cramp, with persistent significant differences between the groups after both real and sham interventions. *Correlate with degree of statistical significant differences (increasing number of asterisks indicates more significant differences). FHD = focal hand dystonia.

motor task. In the sections below, we discuss separately each investigated parameter and the potential inferences.

Cortical excitability and cortical silent period

We found a significantly prolonged cSP in patients with writer's cramp, which is contrary to some of the previous studies demonstrating shortening of cSP in dystonia, implicating disinhibition of the motor cortex being a possible pathophysiological basis for dystonia (Chen *et al.*, 1997, 2017; Curra *et al.*, 2000). Various factors such as stimulus intensity, duration, location and sensory stimulation can influence the duration of cSP, apart from the disorder being studied (Priori *et al.*, 1994; Classen *et al.*, 2000; Ertas *et al.*, 2000; Cantello 2002; Saisanen *et al.*, 2008). The notion of cSP reflective of GABAergic inhibition is based on pharmacological studies showing that drugs affecting GABAergic receptors also change cSP (Priori *et al.*, 1994; Inghilleri *et al.*, 1996). However, a single suprathreshold TMS pulse simultaneously depolarizes all impacted neurons (excitatory, inhibitory, and pyramidal alike), acting as a 'hard reset' of the ongoing subjacent activity. Therefore, the cSP measured in a well controlled experimental set-up could reflect more specifically the time required by the motor circuits to recover and get back to performing a finely regulated motor task (maintaining tonic contraction of FDI muscle) after the artificial depolarization. The prolongation of cSP in writer's cramp could thus indicate a longer duration required for recovery and re-initiation of a finely regulated motor task and not simply disinhibition of the motor cortex.

Premotor-motor interactions

The baseline premotor-motor (PMv-M1) interactions were similar and predominantly inhibitory in both groups, contrary to previous reports for writer's cramp (Houdayer *et al.*, 2012; Pirio Richardson *et al.*, 2017). Our standardized methodology of neuro-navigated targeting of the functionally relevant PMv node during the fine finger tapping task could perhaps explain the differences in the results. Importantly, the real but not the sham cTBS of the dIPL induced a change in the baseline PMv-M1 interaction in the writer's cramp group. Considering the major influence of the parietal lobe on motor cortex is indirect via the premotor cortex (Fagg and Arbib 1998; Bonini *et al.*, 2010, 2012; Schaffelhofer and Scherberger 2016), the change noted in the PMv-M1 interaction after cTBS of dIPL only in patients could suggest the presence of a labile parieto-premotor interaction and the possibility of restoring the normal interactions within the aIPL-PMv-M1 network, as reflected by the restoration of the normal inhibitory aIPL-M1 physiological interaction. In fact, we observed increased functional connectivity between the parietal and premotor regions at rest (dIPL-PMv) in the patients with writer's cramp, before any modulation of the dIPL output.

Parietal-premotor-motor interactions

The baseline influence of dIPL onto M1 was significantly different and opposite between the writer's cramp and healthy volunteers groups: inhibitory in writer's cramp and facilitatory in healthy volunteers. The opposite was noted for the baseline influence of aIPL onto M1: inhibitory in

Table 3 Group comparisons of $cTBS_{dIPL}$ effects in patients with writer's cramp and healthy volunteers

Effect		
cSP	***F***	***P***
Group	31.0	<0.0001
Intervention	0.1	ns
Time	5.2	0.047
Group × Intervention	1.4	ns
Intervention × Time	2.6	ns
Group × Time	0.1	ns
Group × Intervention × Time	0.0	ns
PMv	***F***	***P***
Group	1.0	ns
Intervention	1.9	ns
Time	6.5	0.018
Group × Intervention	0.1	ns
Intervention × Time	2.9	ns
Group × Time	5.6	0.027
Group × Intervention × Time	3.7	0.065
Post hoc	***P***	P_{adj}
Writer's cramp - Real stim: pre versus post	0.0003	0.0012
Writer's cramp - Sham stim: pre versus post	ns	ns
Healthy volunteers - Real stim: pre versus post	ns	ns
Healthy volunteers - Sham stim: pre versus post	ns	ns
aIPL	***F***	***P***
Group	1.04	ns
Intervention	1.35	ns
Time	0.1	ns
Group × Intervention	0.62	ns
Intervention × Time	2.46	ns
Group × Time	5.84	0.023
Group × Intervention × Time	5.33	0.030
Post hoc	***P***	P_{adj}
Writer's cramp, real stim: pre versus post	0.015	0.045
Writer's cramp, sham stim: pre versus post	ns	ns
Healthy volunteers, real stim: pre versus post	ns	ns
Healthy volunteers, sham stim: pre versus post	ns	ns
dIPL	***F***	***P***
Group	29.8	<0.0001

For each of the three outcome measures: cSP, PMV-M1 and aIPL-M1, repeated measures ANOVA was performed to evaluate the effect of group (writer's cramp versus healthy volunteers), intervention (real versus sham) and time (pre- versus post-intervention), and their interactions (Group × Intervention, Group × Time, Intervention × Time, and Group × Intervention × Time). The reported *P*-values were adjusted (Holm's adaptive method) for multiple comparisons for each experiment. For the outcome measure of dIPL-M1, repeated measures ANOVA was performed to evaluate the effect of group (writer's cramp versus healthy volunteers). $cTBS_{dIPL}$ = continuous theta burst stimulation of dIPL; ns = not significant; P_{adj} = *P* adjusted with adaptive Bonferroni-Holm correction.

healthy volunteers, whereas no clear inhibition was found in writer's cramp. The interaction gradient of inhibition-to-facilitation of M1 described in healthy subjects as the conditioning pulse is moved dorsally along the inferior parietal lobe (Karabanov *et al.*, 2013) was absent or inverted in patients with writer's cramp. After cTBS of dIPL node, the abnormal null influence of the aIPL onto M1 was restored towards the normal inhibitory interaction observed in healthy volunteers, suggestive of functional interactions within the IPL, which can have downstream influence on the fine motor control network.

An analogy can be made between our understanding of the development of motor skills for the performance of various tasks and development of language vocabulary, as the development of a motor vocabulary. Task-specific dystonia such as writer's cramp can be viewed as the inability to execute a particular motor task secondary to the corruption of the motor vocabulary, although the concept and the skills required for the performance of the task seem intact. The aberrant downstream influence of the multimodal sensory integration region is optimally positioned to corrupt the execution of a learned motor skill. The aberrancies introduced into the motor command can clinically manifest variously as abnormal dystonic adaptations characterized by dystonic posturing, cramping, difficulty to maintain a stable grip, tremors or sudden interruptions or 'blocks' in ongoing activity.

Limitations

Our study could have benefited from a larger cohort. However, the results rely on a clinically homogenous pool of patients, matched controls, and a highly personalized approach. The precise targeting based on functionally relevant hubs and individual anatomy prevented the inherent problem of targeting based on aggregated atlas coordinates. Also, the sham-controlled cross-over design of the study allowed us (i) to maximize the outcome by measuring real and sham stimulation effects in every subject; and (ii) to confirm the reliability of electrophysiological parameters by measuring them in two separate sessions, before each intervention. Patients with writer's cramp exhibit a complex psychopathological profile that could influence the detection of neural differences (Sadnicka *et al.*, 2018), especially in the dynamic state. We believe the resting state evaluation of the experimental outcomes noted in this study is another major strength, since the network abnormalities could be more reflective of the disease pathophysiology rather than an epiphenomenon of the dystonic state.

This study did not quantify changes in clinical scores for two main reasons: (i) because of the limited time available to explore the electrophysiological interactions post-cTBS; and (ii) because we did not expect *a priori* any significant clinical effects. Early studies used single session inhibitory repetitive TMS over the M1 or PMv as a proof of concept (Siebner *et al.*, 1999; Murase *et al.*, 2005), and their conclusions were subsequently leveraged in studies using stimulations over longer periods combined with other interventions (Borich *et al.*, 2009; Kimberley *et al.*, 2015; Pirio Richardson *et al.*, 2017). A single session of TBS is unlikely to induce any lasting clinically-relevant effect due to the very nature of this pathology (Meunier *et al.*, 2015), in which long abnormal training changes the circuitry supporting a specific fine motor task (Sadnicka *et al.*, 2018).

In conclusion, these findings put the spotlight on the abnormal multilateral interactions between the parietal,

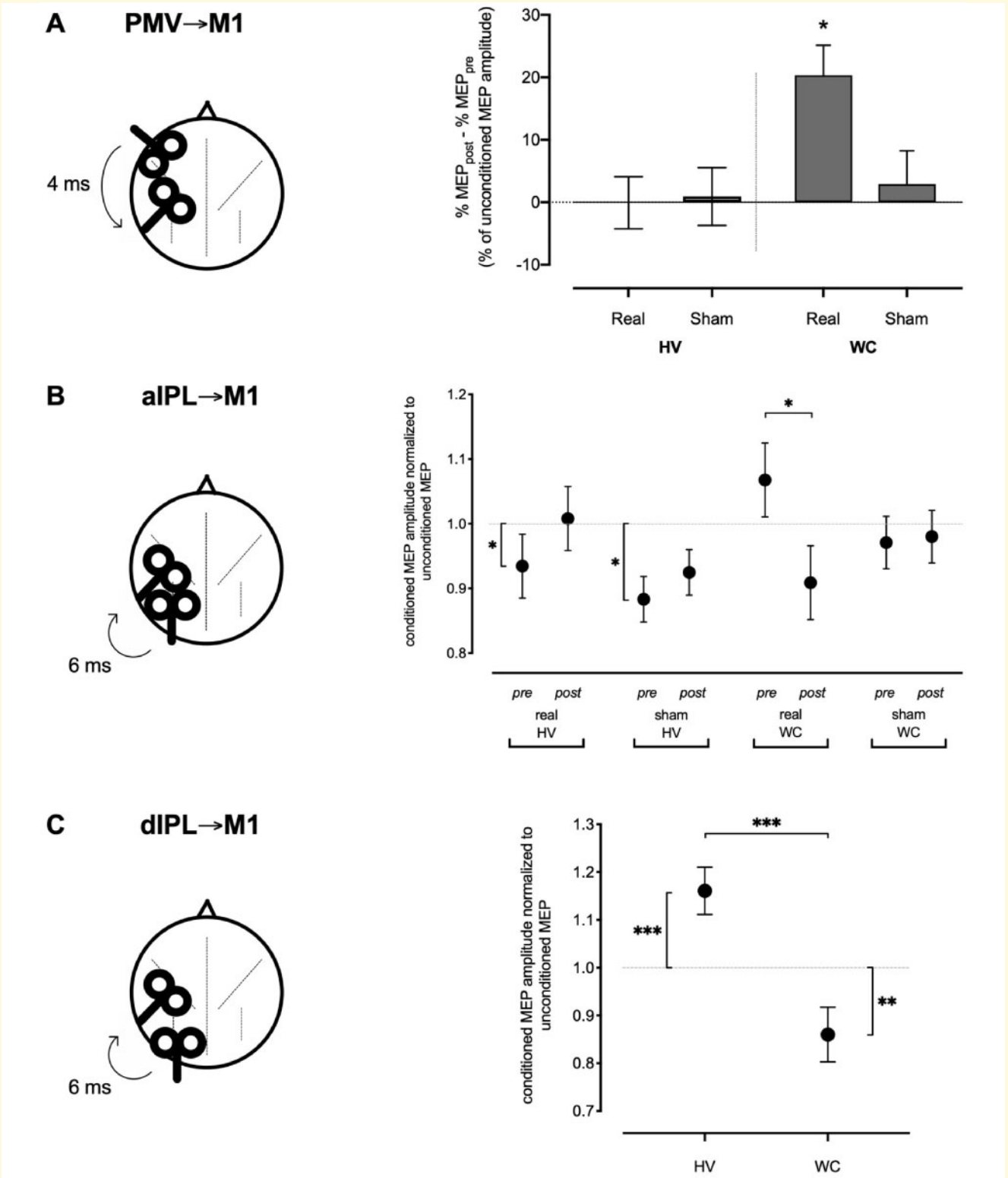

Figure 5 Summary of TMS results. (**A**) Changes in the PMv-M1 electrophysiological interaction (ISI 4 ms) introduced by real or sham $cTBS_{dlPL}$ in healthy volunteers (HV) and writer's cramp (WC) groups. The changes are represented as the difference between conditioned MEP amplitudes normalized to the unconditioned MEP amplitudes after versus before the intervention. The changes were significant only in the writer's cramp group after the real $cTBS_{dlPL}$. (**B**) Changes in the aIPL-M1 electrophysiological interaction (ISI 6 ms) introduced by real or sham $cTBS_{dlPL}$ in healthy volunteers and writer's cramp groups. The conditioned MEP amplitudes are represented normalized to the unconditioned ones. At baseline, the aIPL-M1 was significantly inhibitory only in the healthy volunteers and without modulatory effect in writer's cramp. The interaction changed to inhibitory only after the real stimulation in writer's cramp. No significant change was noted after either real or sham intervention in healthy volunteers, or after sham intervention in writer's cramp group. (**C**) The baseline dlPL-M1 interaction (influence of conditioning stimulus to dlPL given 6 ms preceding M1 stimulation) was significantly facilitatory for the healthy volunteers group and significantly inhibitory for the writer's cramp group.

premotor, and motor cortices in the generation of writer's cramp. They also provide a potential point of entry for re-establishing the normal dynamics in this network. The behavioural implications of restoring these physiological aberrancies and the potential therapeutic implications of modulating the influence of the parietal multimodal sensory integration region needs further exploration.

Acknowledgements

We would like to thank Binquan Wang for providing assistance with the initial MRI scans, Ms Nguyet Dang for help with experimental set-up and Ms Elaine Considine, RN and Dr Ejaz Shamim for assistance with patient recruitment.

Funding

This research was supported by the Intramural Research Programs of the NIH, National Institute of Neurological Disorders and Stroke and National Center for Complementary and Integrative Health and Dystonia Medical Research Foundation.

Competing interests

The authors report no competing interests.

Supplementary material

Supplementary material is available at *Brain* online.

References

Albanese A, Bhatia K, Bressman SB, Delong MR, Fahn S, Fung VS, et al. Phenomenology and classification of dystonia: a consensus update'. Mov Disord 2013; 28: 863–73.

Battistella G, Simonyan K. Top-down alteration of functional connectivity within the sensorimotor network in focal dystonia'. Neurology 2019; 92: e1843–e51.

Battistella G, Termsarasab P, Ramdhani RA, Fuertinger S, Simonyan K. Isolated focal dystonia as a disorder of large-scale functional networks. Cereb Cortex 2017; 27: 1203–15.

Baumer T, Schippling S, Kroeger J, Zittel S, Koch G, Thomalla G, et al. Inhibitory and facilitatory connectivity from ventral premotor to primary motor cortex in healthy humans at rest–a bifocal TMS study. Clin Neurophysiol 2009; 120: 1724–31.

Bianchi S, Fuertinger S, Huddleston H, Frucht SJ, Simonyan K. Functional and structural neural bases of task specificity in isolated focal dystonia. Mov Disord 2019; 34: 555–63.

Bonini L, Rozzi S, Serventi FU, Simone L, Ferrari PF, Fogassi L. Ventral premotor and inferior parietal cortices make distinct contribution to action organization and intention understanding. Cereb Cortex 2010; 20: 1372–85.

Bonini L, Ugolotti Serventi F, Bruni S, Maranesi M, Bimbi M, Simone L, et al. Selectivity for grip type and action goal in macaque inferior parietal and ventral premotor grasping neurons. J Neurophysiol 2012; 108: 1607–19.

Borich M, Arora S, Kimberley TJ. Lasting effects of repeated rTMS application in focal hand dystonia. Restor Neurol Neurosci 2009; 27: 55–65.

Bremmer F, Schlack A, Shah NJ, Zafiris O, Kubischik M, Hoffmann K, et al. Polymodal motion processing in posterior parietal and premotor cortex: a human fMRI study strongly implies equivalencies between humans and monkeys. Neuron 2001; 29: 287–96.

Bruni S, Gerbella M, Bonini L, Borra E, Coude G, Ferrari PF, et al. Cortical and subcortical connections of parietal and premotor nodes of the monkey hand mirror neuron network. Brain Struct Funct 2018; 223: 1713–29.

Burke RE, Fahn S, Marsden CD, Bressman SB, Moskowitz C, Friedman J. Validity and reliability of a rating scale for the primary torsion dystonias. Neurology 1985; 35: 73–7.

Burks JD, Boettcher LB, Conner AK, Glenn CA, Bonney PA, Baker CM, et al. White matter connections of the inferior parietal lobule: a study of surgical anatomy. Brain Behav 2017; 7: e00640.

Cantello R. Prolonged cortical silent period after transcranial magnetic stimulation in generalized epilepsy. Neurology 2002; 58: 1135; author reply 35.

Caspers S, Schleicher A, Bacha-Trams M, Palomero-Gallagher N, Amunts K, Zilles K. Organization of the human inferior parietal lobule based on receptor architectonics. Cereb Cortex 2013; 23: 615–28.

Cerri G, Shimazu H, Maier MA, Lemon RN. Facilitation from ventral premotor cortex of primary motor cortex outputs to macaque hand muscles. J Neurophysiol 2003; 90: 832–42.

Chen M, Summers RL, Goding GS, Samargia S, Ludlow CL, Prudente CN, et al. Evaluation of the cortical silent period of the laryngeal motor cortex in healthy individuals. Front Neurosci 2017; 11: 88.

Chen R, Wassermann EM, Canos M, Hallett M. Impaired inhibition in writer's cramp during voluntary muscle activation. Neurology 1997; 49: 1054–9.

Classen J, Steinfelder B, Liepert J, Stefan K, Celnik P, Cohen LG, et al. Cutaneomotor integration in humans is somatotopically organized at various levels of the nervous system and is task dependent. Exp Brain Res 2000; 130: 48–59.

Curra A, Romaniello A, Berardelli A, Cruccu G, Manfredi M. Shortened cortical silent period in facial muscles of patients with cranial dystonia. Neurology 2000; 54: 130–5.

Davare M, Lemon R, Olivier E. Selective modulation of interactions between ventral premotor cortex and primary motor cortex during precision grasping in humans. J Physiol 2008; 586: 2735–42.

Deroche MLD, Nguyen DL, Gracco VL. Modulation of speech motor learning with transcranial direct current stimulation of the inferior parietal lobe. Front Integr Neurosci 2017; 11: 35.

Economo C, Koskinas GN. Die cytoarchitektonik der hirnrinde des erwachsenen menschen. Wien und Berlin: J. Springer; 1925.

Ertas NK, Gul G, Altunhalka A, Kirbas D. Cortical silent period following transcranial magnetic stimulation in epileptic patients. Epileptic Disord 2000; 2: 137–40.

Fagg AH, Arbib MA. Modeling parietal-premotor interactions in primate control of grasping. Neural Netw 1998; 11: 1277–303.

Gallea C, Horovitz SG, Najee-Ullah M, Hallett M. Impairment of a parieto-premotor network specialized for handwriting in writer's cramp. Hum Brain Mapp 2016; 37: 4363–75.

Grafton ST, Fagg AH, Arbib MA. Dorsal premotor cortex and conditional movement selection: a PET functional mapping study. J Neurophysiol 1998; 79: 1092–7.

Hallett M. Neurophysiology of dystonia: the role of inhibition. Neurobiol Dis 2011; 42: 177–84.

Hamano YH, Sugawara SK, Yoshimoto T, Sadato N. The motor engram as a dynamic change of the cortical network during early sequence learning: An fMRI study. Neurosci Res 2020; 153: 27–39.

Houdayer E, Beck S, Karabanov A, Poston B, Hallett M. The differential modulation of the ventral premotor-motor interaction during movement initiation is deficient in patients with focal hand dystonia. Eur J Neurosci 2012; 35: 478–85.

Huang YZ, Edwards MJ, Rounis E, Bhatia KP, Rothwell JC. Theta burst stimulation of the human motor cortex. Neuron 2005; 45: 201–6.
Hubsch C, Roze E, Popa T, Russo M, Balachandran A, Pradeep S, et al. Defective cerebellar control of cortical plasticity in writer's cramp. Brain 2013; 136: 2050–62.
Inghilleri M, Berardelli A, Marchetti P, Manfredi M. Effects of diazepam, baclofen and thiopental on the silent period evoked by transcranial magnetic stimulation in humans'. Exp Brain Res 1996; 109: 467–72.
Irfanoglu MO, Nayak A, Jenkins J, Pierpaoli C. TORTOISE v3: Improvements and new features of the NIH diffusion MRI processing pipeline. In: Program and proceedings of the ISMRM 25th annual meeting and exhibition, Honolulu, HI, USA, 2017. Abstract #3540.
Ishibashi R, Lambon Ralph MA, Saito S, Pobric G. Different roles of lateral anterior temporal lobe and inferior parietal lobule in coding function and manipulation tool knowledge: evidence from an rTMS study. Neuropsychologia 2011; 49: 1128–35.
Kaji R, Bhatia K, Graybiel AM. Pathogenesis of dystonia: is it of cerebellar or basal ganglia origin? J Neurol Neurosurg Psychiatry 2018; 89: 488–92.
Karabanov A, Jin SH, Joutsen A, Poston B, Aizen J, Ellenstein A, et al. Timing-dependent modulation of the posterior parietal cortex-primary motor cortex pathway by sensorimotor training. J Neurophysiol 2012; 107: 3190–9.
Karabanov AN, Chao CC, Paine R, Hallett M. Mapping different intra-hemispheric parietal-motor networks using twin Coil TMS. Brain Stimul 2013; 6: 384–9.
Kimberley TJ, Schmidt RL, Chen M, Dykstra DD, Buetefisch CM. Mixed effectiveness of rTMS and retraining in the treatment of focal hand dystonia. Front Hum Neurosci 2015; 9: 385.
Koch G, Fernandez Del Olmo M, Cheeran B, Schippling S, Caltagirone C, Driver J, et al. Functional interplay between posterior parietal and ipsilateral motor cortex revealed by twin-coil transcranial magnetic stimulation during reach planning toward contralateral space. J Neurosci 2008; 28: 5944–53.
Kristo G, Rutten GJ, Raemaekers M, de Gelder B, Rombouts SA, Ramsey NF. Task and task-free FMRI reproducibility comparison for motor network identification. Hum Brain Mapp 2014; 35: 340–52.
Lemon RN. Descending pathways in motor control. Annu Rev Neurosci 2008a; 31: 195–218.
Lemon RN. An enduring map of the motor cortex. Exp Physiol 2008b; 93: 798–802.
Mayka MA, Corcos DM, Leurgans SE, Vaillancourt DE. Three-dimensional locations and boundaries of motor and premotor cortices as defined by functional brain imaging: a meta-analysis. Neuroimage 2006; 31: 1453–74.
Meunier S, Popa T, Hubsch C, Roze E, Kishore A. Reply: A single session of cerebellar theta burst stimulation does not alter writing performance in writer's cramp. Brain 2015; 138: e356.
Murase N, Rothwell JC, Kaji R, Urushihara R, Nakamura K, Murayama N, et al. Subthreshold low-frequency repetitive transcranial magnetic stimulation over the premotor cortex modulates writer's cramp. Brain 2005; 128: 104–15.
Peterson DA, Sejnowski TJ, Poizner H. Convergent evidence for abnormal striatal synaptic plasticity in dystonia. Neurobiol Dis 2010; 37: 558–73.
Pierpaoli C. Quantitative Brain MRI. Top Magn Reson Imaging 2010; 21: 63.
Pirio Richardson S, Altenmuller E, Alter K, Alterman RL, Chen R, Frucht S, et al. Research priorities in limb and task-specific dystonias. Front Neurol 2017; 8: 170.
Priori A, Berardelli A, Inghilleri M, Accornero N, Manfredi M. Motor cortical inhibition and the dopaminergic system. Pharmacological changes in the silent period after transcranial brain stimulation in normal subjects, patients with Parkinson's disease and drug-induced parkinsonism. Brain 1994; 117 (Pt 2): 317–23.
Quartarone A, Hallett M. Emerging concepts in the physiological basis of dystonia. Mov Disord 2013; 28: 958–67.
Rizzolatti G, Luppino G. The cortical motor system. Neuron 2001; 31: 889–901.
Rizzolatti G, Wolpert DM. Motor systems. Curr Opin Neurobiol 2005; 15: 623–5.
Rozzi S, Ferrari PF, Bonini L, Rizzolatti G, Fogassi L. Functional organization of inferior parietal lobule convexity in the macaque monkey: electrophysiological characterization of motor, sensory and mirror responses and their correlation with cytoarchitectonic areas. Eur J Neurosci 2008; 28: 1569–88.
Saad ZS, Reynolds RC. Suma. Neuroimage 2012; 62: 768–73.
Sadnicka A, Kassavetis P, Parees I, Meppelink AM, Butler K, Edwards M. Task-specific dystonia: pathophysiology and management. J Neurol Neurosurg Psychiatry 2016; 87: 968–74.
Sadnicka A, Kornysheva K, Rothwell JC, Edwards MJ. A unifying motor control framework for task-specific dystonia. Nat Rev Neurol 2018; 14: 116–24.
Saisanen L, Pirinen E, Teitti S, Kononen M, Julkunen P, Maatta S, et al. Factors influencing cortical silent period: optimized stimulus location, intensity and muscle contraction. J Neurosci Methods 2008; 169: 231–8.
Schaffelhofer S, Scherberger H. 'Object vision to hand action in macaque parietal, premotor, and motor cortices. Elife 2016; eLife.15278.
Shakkottai VG, Batla A, Bhatia K, Dauer WT, Dresel C, Niethammer M, et al. Current opinions and areas of consensus on the role of the cerebellum in dystonia. Cerebellum 2017; 16: 577–94.
Shimazu H, Maier MA, Cerri G, Kirkwood PA, Lemon RN. Macaque ventral premotor cortex exerts powerful facilitation of motor cortex outputs to upper limb motoneurons. J Neurosci 2004; 24: 1200–11.
Shrout PE, Fleiss JL. Intraclass correlations - uses in assessing rater reliability. Psychol Bull 1979; 86: 420–8.
Siebner HR, Auer C, Ceballos-Baumann A, Conrad B. Has repetitive transcranial magnetic stimulation of the primary motor hand area a therapeutic application in writer's cramp? Electroencephalogr Clin Neurophysiol Suppl 1999; 51: 265–75.
Taylor PA, Saad ZS. FATCAT: (an efficient) Functional and Tractographic Connectivity Analysis Toolbox. Brain Connect 2013; 3: 523–35.
Wischnewski M, Schutter D. Efficacy and time course of paired associative stimulation in cortical plasticity: implications for neuropsychiatry. Clin Neurophysiol 2016; 127: 732–9.